NASA Technical Memorandum 4535

Mechanical and Thermal Buckling Analysis of Sandwich Panels Under Different Edge Conditions

William L. Ko
Dryden Flight Research Facility
Edwards, California

National Aeronautics and
Space Administration
Office of Management
Scientific and Technical
Information Program
1993

MECHANICAL AND THERMAL BUCKLING ANALYSIS OF SANDWICH PANELS UNDER DIFFERENT EDGE CONDITIONS

William L. Ko
NASA Dryden Flight Research Facility
Edwards, California 93523-0273
United States of America

ABSTRACT

By using the Rayleigh-Ritz method of minimizing the total potential energy of a structural system, combined load (mechanical or thermal load) buckling equations are established for orthotropic rectangular sandwich panels supported under four different edge conditions. Two-dimensional buckling interaction curves and three-dimensional buckling interaction surfaces are constructed for high-temperature honeycomb-core sandwich panels supported under four different edge conditions. The interaction surfaces provide easy comparison of the panel buckling strengths and the domains of symmetrical and antisymmetrical buckling associated with the different edge conditions. Thermal buckling curves of the sandwich panels also are presented. The thermal buckling conditions for the cases with and without thermal moments were found to be identical for the small deformation theory. In sandwich panels, the effect of transverse shear is quite large, and by neglecting the transverse shear effect, the buckling loads could be overpredicted considerably. Clamping of the edges could greatly increase buckling strength more in compression than in shear.

KEYWORDS Sandwich panels; Mechanical buckling; Thermal buckling; Buckling interaction surfaces; Buckling interaction curves.

NOMENCLATURE

A_{mn}	Fourier coefficients of trial function for w, in.
$\bar{A}_{ij}$	extensional stiffnesses of sandwich panel, lb/in.
a	length of sandwich panel, in.
a_o	edge length of square sandwich panel, in.
$a^{ij}_{mnk\ell}$	coefficients of characteristic equations
B_{mn}	Fourier coefficients of trial function for γ_{xz}, in./in.
b	width of sandwich panel, in.
C_{mn}	Fourier coefficients of trial function for γ_{yz}, in./in.
D_{ij}	bending stiffnesses of sandwich panel, in-lb
D_{Qx}, D_{Qy}	transverse shear stiffnesses in xz, yz planes, lb/in.
D^*	flexural stiffness parameters, $\sqrt{D_{11}D_{22}}$, in-lb
E_x, E_y	Young's moduli of face sheets, lb/in^2
G_{Cxz}, G_{Cyz}	effective transverse shear moduli of honeycomb core, lb/in^2
G_{xy}	shear modulus of face sheets, lb/in^2
h	depth of sandwich panel = distance between middle surfaces of two face sheets, in.
h_c	depth of honeycomb core, $h_c = h - t_s$, in.
I_s	moment of inertia, per unit width, of a face sheet taken with respect to horizontal centroidal axis of the sandwich panel, $I_s = \frac{1}{4}t_s h^2 + \frac{1}{12}t_s^3$, in^4/in.
i	index, 1, 2, 3, $\cdots$
j	index, 1, 2, 3, $\cdots$
k	index, 1, 2, 3, $\cdots$
k_x, k_y	compressive buckling load factors in x- and y-directions, $k_x = \frac{N_x a^2}{\pi^2 D^*}$, $k_y = \frac{N_y a^2}{\pi^2 D^*}$, for a = constant
k_{xy}	shear buckling factor, $k_{xy} = \frac{N_{xy} a^2}{\pi^2 D^*}$, for a = constant
$\bar{k}_x, \bar{k}_y$	modified compressive buckling load factors in x- and y-directions, $\bar{k}_x = \frac{N_x a_o^2}{\pi^2 D^*} = k_x \frac{b}{a}$, $\bar{k}_y = \frac{N_y a_o^2}{\pi^2 D^*} = k_y \frac{b}{a}$, for $ab = a_o^2$ = constant
$\bar{k}_{xy}$	modified shear buckling load factor, $\bar{k}_{xy} = \frac{N_{xy} a_o^2}{\pi^2 D^*} = k_{xy}\frac{b}{a}$, for $ab = a_o^2$ = constant
ℓ	index, 1, 2, 3, $\cdots$
M_x, M_y	bending moment intensities, (in-lb)/in.
M_{xy}	twisting moment intensity, (in-lb)/in.

M_x^T, M_y^T, M_{xy}^T	thermal moments, (in-lb)/in.
m	number of buckle half waves in x-direction
N_x, N_y	normal stress resultants, lb/in.
N_{xy}	shear stress resultant, lb/in.
N_x^T, N_y^T, N_{xy}^T	thermal forces, lb/in.
n	number of buckle half waves in y-direction
Q_x, Q_y	transverse shear force intensities, lb/in.
T	temperature, °F
T_{cr}	critical buckling temperature, °F
t_s	thickness of sandwich face sheets, in.
V	total potential energy of sandwich panel, in-lb
V_1	strain energy of sandwich panel, in-lb
V_2	work done by external forces, in-lb
u, v, w	middle surface displacement components in x-, y-, and z-direction, in.
x, y, z	rectangular Cartesian coordinates
$\alpha_x, \alpha_y, \alpha_{xy}$	coefficients of thermal expansion, in/in-°F
γ_{xz}, γ_{yz}	transverse shear strains in xz- and yz-plane, in./in.
ζ	numerical coefficient of N_y^T in a_{mnkl}^{11}
η	numerical factor in buckling equation, and associated with an edge condition
ξ	numerical coefficient of N_x^T in a_{mnkl}^{11}
ν_{xy}, ν_{yz}	Poisson ratios of face sheets, also used for those of sandwich panel

INTRODUCTION

The structural components of hypersonic flight vehicles (e.g., spacecraft, rockets, reentry vehicles, aircraft, etc.) are subjected to hyperthermal loadings caused by hostile aerodynamic heating during ascent and reentry, or caused by solar radiation during spaceflight. These structural components have to operate at elevated temperatures and, therefore, are called hot structures. Because of nonuniform heating (which is magnified by the cooler substructural frames that act as heat sinks) and the mechanical structural constraints, severe thermal stresses could build up in those hot structures. Excess thermal loading may induce material degradation, thermal creep, thermal yielding, thermal buckling, thermal crack fracture after cool down, etc. Any disruption of the surface smoothness of these structures (e.g., metallic thermal protection system (ref. 1) or hypersonic aircraft engine inlet structures (refs. 2, 3), etc.) caused by the above failure modes, especially thermal buckling, could disturb the flow field, creating hot spots that could cause very serious consequences to the structures. Thus, the thermal load is a key factor in the design of hot structures. Reference 1 discusses various design concepts of both hot and cryogenic structural components for hypersonic flight vehicles. The potential candidates of high-buckling-strength hot-structural panels (fabricated with superalloys) for hypersonic aircraft applications are tubular panels, beaded panels, truss-core sandwich panels, hat-stiffened panels, honeycomb-core sandwich panels, etc. (refs. 4, 5). The combined-load buckling behavior of tubular panels was studied by Ko et al. (ref. 4) extensively both theoretically and experimentally. The compressive buckling characteristics of the beaded panels were investigated by Siegel (ref. 5).

Recently Ko and Jackson (ref. 6) and Percy and Fields (ref. 7) studied the compressive buckling behavior of a hat-stiffened panel designed for application to the hypersonic aircraft fuselage skin panel. Furthermore, Ko and Jackson conducted simple analysis of thermal behavior (thermal buckling of face sheet) of a honeycomb-core sandwich panel (ref. 8) and compared the relative combined-load buckling strengths of truss-core and honeycomb-core sandwich panels (ref. 9). They also investigated the effect of fiber orientation of a metal-matrix face sheet on the combined-load buckling strength of honeycomb-core sandwich panels (refs. 10, 11). Most of the past mechanical buckling analyses of sandwich panels (refs. 4–7 and 9–12) and flat plates (refs. 13, 14) were conducted for simply supported edge conditions because the analysis was mathematically less involved. For the case of clamped edge conditions, Green and Hearmon (ref. 15) studied combined loading stability of plywood plates, and Smith (ref. 16) considered only pure shear buckling of the plywood plates. Kuenzi, Erickson, and Zahn (ref. 17) considered also shear stability of flat panels of sandwich construction. The workers cited here ignored the transverse shear effect in their analyses. King (ref. 18) analyzed the stability of clamped rectangular sandwich plates subjected to in-plane combined loadings, taking into account the rotational effect of the sandwich core. A less-compact displacement function (that could be reduced to a simpler Green and Hearmon displacement function (ref. 15)) was used, resulting in a very complicated expression for the potential energy of the sandwich system. Most of the past thermal buckling analysis was done on single plates (refs. 19–22) or laminated composite plates (refs. 23–27), for which the transverse shear effect may be neglected. In the actual application of hot structural panels, most panel boundary conditions are closer to the clamped edges rather than the simply supported edges. Therefore, this paper will consider the combined-load mechanical and thermal buckling of sandwich panels under different types of edge conditions by taking into account the transverse shear effect, and will compare the buckling interaction curves and surfaces for different edge conditions.

DESCRIPTION OF PROBLEM

Figure 1 shows the geometry of a rectangular honeycomb-core sandwich panel having identical face sheets. The extensional and bending stiffnesses of the panel will be provided by the two face sheets only, and the transverse shear stiffnesses by the honeycomb core only.

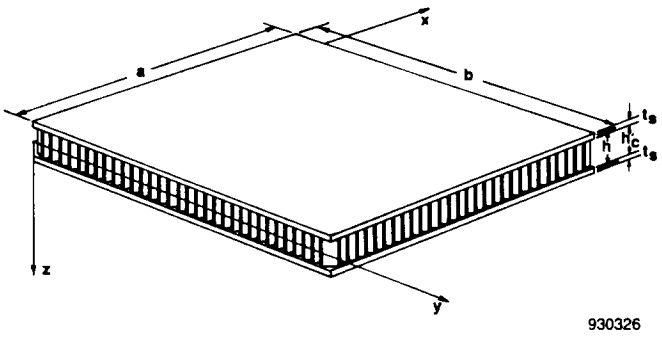

Fig. 1. A honeycomb-core sandwich panel.

This type of sandwich panel, when fabricated with high-temperature alloy (e.g., titanium alloy), becomes the so-called hot structure and could be a potential candidate for hypersonic aircraft structural applications (ref. 1). Figure 2 shows the sandwich panel subjected to combined compressive and shear loadings in its middle plane. The conventional Rayleigh-Ritz method of minimizing the panel total potential energy will be used in the combined-load buckling analysis, accounting for the transverse shear effect (fig. 3). The sandwich panel will be supported under four different edge conditions:

- Case 1: Four edges simply supported (4S edge condition)
- Case 2: Four edges clamped (4C edge condition)
- Case 3: Two sides clamped, two ends simply supported (2C2S edge condition)
- Case 4: Two sides simply supported, two ends clamped (2S2C edge condition)

where the sides and ends are parallel to the x- and y-axes, respectively.

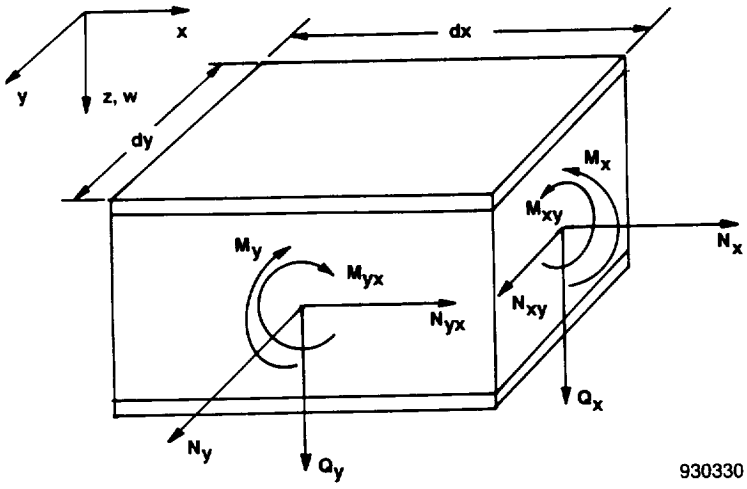

Fig. 2. Forces and moments acting on differential element of a sandwich panel.

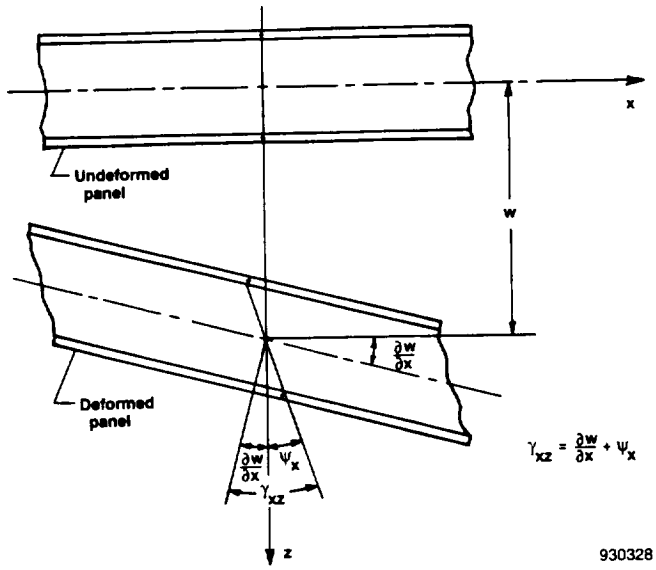

Fig. 3. Deformation of a sandwich panel in xz-plane.

The problem is to study the effects of the panel edge condition and the panel aspect ratio on the combined-load buckling behavior of the sandwich panel. Case 1 has already been solved and was published in reference 9. For completeness, however, some key equations for Case 1 will be repeated in this paper.

GOVERNING EQUATIONS

Constitutive Equations

For the classical orthotropic thick plate theory, the thermoelastic constitutive equations for membrane forces, moments, and the transverse shear constitutive equation may be written as (fig. 2)

$$\begin{bmatrix} N_x \\ N_y \\ N_{xy} \end{bmatrix} = \begin{bmatrix} \bar{A}_{11} & \bar{A}_{12} & 0 \\ \bar{A}_{21} & \bar{A}_{22} & 0 \\ 0 & 0 & \bar{A}_{66} \end{bmatrix} \begin{bmatrix} \frac{\partial u}{\partial x} \\ \frac{\partial u}{\partial y} \\ \frac{\partial u}{\partial y} + \frac{\partial v}{\partial x} \end{bmatrix} - \begin{bmatrix} N_x^T \\ N_y^T \\ N_{xy}^T \end{bmatrix} \tag{1}$$

$$\begin{bmatrix} M_x \\ M_y \\ M_{xy} \end{bmatrix} = \begin{bmatrix} D_{11} & D_{12} & 0 \\ D_{21} & D_{22} & 0 \\ 0 & 0 & D_{66} \end{bmatrix} \times \begin{bmatrix} -\frac{\partial}{\partial x}\left(\frac{\partial w}{\partial x} - \gamma_{xz}\right) \\ -\frac{\partial}{\partial y}\left(\frac{\partial w}{\partial y} - \gamma_{yz}\right) \\ -\frac{\partial}{\partial y}\left(\frac{\partial w}{\partial x} - \gamma_{xz}\right) - \frac{\partial}{\partial x}\left(\frac{\partial w}{\partial y} - \gamma_{yz}\right) \end{bmatrix} - \begin{bmatrix} M_x^T \\ M_y^T \\ M_{xy}^T \end{bmatrix} \tag{2}$$

$$\begin{bmatrix} Q_x \\ Q_y \end{bmatrix} = \begin{bmatrix} D_{Qx} & 0 \\ 0 & D_{Qy} \end{bmatrix} \begin{bmatrix} \gamma_{xz} \\ \gamma_{yz} \end{bmatrix} \tag{3}$$

For the sandwich panel whose extensional and bending stiffnesses are provided only by the two identical face sheets, and the transverse shear stiffnesses only by the honeycomb core, the extensional and the bending stiffnesses $\{\bar{A}_{ij}, D_{ij}\}$ in equations (1) and (2), and the transverse shear stiffnesses $\{D_{Qx}, D_{Qy}\}$ in equation (3) may be written as

$$\begin{bmatrix} \bar{A}_{11} & , & D_{11} \\ \bar{A}_{12} & , & D_{12} \\ \bar{A}_{21} & , & D_{21} \\ \bar{A}_{22} & , & D_{22} \\ \bar{A}_{66} & , & D_{66} \end{bmatrix} = [2t_s,\ 2I_s] \begin{bmatrix} \frac{E_x}{1-\nu_{xy}\nu_{yx}} \\ \frac{\nu_{yx}E_x}{1-\nu_{xy}\nu_{yx}} \\ \frac{\nu_{xy}E_y}{1-\nu_{xy}\nu_{yx}} \\ \frac{E_y}{1-\nu_{xy}\nu_{yx}} \\ G_{xy} \end{bmatrix} \tag{4}$$

$$\begin{bmatrix} D_{Qx} \\ D_{Qy} \end{bmatrix} = [h_c] \begin{bmatrix} G_{Cxz} \\ G_{Cyz} \end{bmatrix} \tag{5}$$

where the 2 in front of $\{t_s, I_s\}$ in equation (4) is associated with two identical face sheets.

The thermal forces $\{N_x^T, N_y^T, N_{xy}^T\}$ and the thermal moments $\{M_x^T, M_y^T, M_{xy}^T\}$ appearing in equations (1) and (2) are defined by:

$$\begin{bmatrix} N_x^T & , & M_x^T \\ N_y^T & , & M_y^T \\ N_{xy}^T & , & M_{xy}^T \end{bmatrix} = \sum_{i=1}^{2} \left\{ \begin{bmatrix} t_s\ T_i, & (-1)^i \frac{t_s h}{2}\ T_i \end{bmatrix} \times \begin{bmatrix} \frac{E_x}{1-\nu_{xy}\nu_{yx}} & \frac{\nu_{yx}E_x}{1-\nu_{xy}\nu_{yx}} & 0 \\ \frac{\nu_{xy}E_y}{1-\nu_{xy}\nu_{yx}} & \frac{E_y}{1-\nu_{xy}\nu_{yx}} & 0 \\ 0 & 0 & G_{xy} \end{bmatrix}_i \begin{bmatrix} \alpha_x \\ \alpha_y \\ \alpha_{xy} \end{bmatrix}_i \right\} \tag{6}$$

where $i = 1, 2$ are associated, respectively, with the lower and the upper face sheets, and $[\,]_i$ $(i = 1, 2)$ implies that the material properties are associated with temperature T_i $(i = 1, 2)$. The thermal force and thermal moment contributions from the honeycomb core were neglected.

Energy Equations

Based on the small deformation theory, the strain energy V_1 of the heated sandwich panel may be written as (refs. 23, 24, 26, 27)

$$\begin{aligned} V_1 = \int_o^a \int_o^b \Bigg\{ & \frac{A_{11}}{2}\left(\frac{\partial u}{\partial x}\right)^2 + A_{12}\left(\frac{\partial u}{\partial x}\right)\left(\frac{\partial v}{\partial y}\right) + \frac{A_{22}}{2}\left(\frac{\partial v}{\partial y}\right)^2 \\ & + \frac{A_{66}}{2}\left(\frac{\partial u}{\partial y} + \frac{\partial v}{\partial x}\right)^2 + \frac{D_{11}}{2}\left[\frac{\partial}{\partial x}\left(\frac{\partial w}{\partial x} - \gamma_{xz}\right)\right]^2 \\ & + D_{12}\left[\frac{\partial}{\partial x}\left(\frac{\partial w}{\partial x} - \gamma_{xz}\right)\right]\left[\frac{\partial}{\partial y}\left(\frac{\partial w}{\partial y} - \gamma_{yz}\right)\right] \\ & + \frac{D_{22}}{2}\left[\frac{\partial}{\partial y}\left(\frac{\partial w}{\partial y} - \gamma_{yz}\right)\right]^2 \\ & + \frac{D_{66}}{2}\left[\frac{\partial}{\partial y}\left(\frac{\partial w}{\partial x} - \gamma_{xz}\right) + \frac{\partial}{\partial x}\left(\frac{\partial w}{\partial y} - \gamma_{yz}\right)\right]^2 + \frac{D_{Qx}}{2}\gamma_{xz}^2 + \frac{D_{Qy}}{2}\gamma_{yz}^2 \\ & - N_x^T\left(\frac{\partial u}{\partial x}\right) - N_{xy}^T\left(\frac{\partial u}{\partial y} + \frac{\partial v}{\partial x}\right) - N_y^T\left(\frac{\partial v}{\partial y}\right) \\ & + M_x^T\left[\frac{\partial}{\partial x}\left(\frac{\partial w}{\partial x} - \gamma_{xz}\right)\right] + M_y^T\left[\frac{\partial}{\partial x}\left(\frac{\partial w}{\partial y} - \gamma_{yz}\right)\right] \\ & + M_{xy}^T\left[\frac{\partial}{\partial y}\left(\frac{\partial w}{\partial x} - \gamma_{xz}\right) + \frac{\partial}{\partial x}\left(\frac{\partial w}{\partial y} - \gamma_{yz}\right)\right] \Bigg\} dxdy \end{aligned} \tag{7}$$

← energy terms for mechanical buckling

For the buckling problem, the work done V_2 by the in-plane forces to produce transverse deflection is given by

$$V_2 = \frac{1}{2}\int_o^a \int_o^b \left[N_x\left(\frac{\partial w}{\partial x}\right)^2 + 2N_{xy}\left(\frac{\partial w}{\partial x}\right)\left(\frac{\partial w}{\partial y}\right) + N_y\left(\frac{\partial w}{\partial y}\right)^2 \right] dxdy \tag{8}$$

The total potential energy V of the sandwich panel is then $V = V_1 + V_2$.

Panel Boundary Conditions

The sandwich panel is to be supported at its four edges under the following four cases of boundary conditions:

For mechanical buckling:

Case 1. 4S edge condition: $x = 0, a:\ w = M_x = \gamma_{yz} = 0$; $y = 0, b: w = M_y = \gamma_{xz} = 0$

Case 2. 4C edge condition: $x = 0, a:\ w = \frac{\partial w}{\partial x} = \gamma_{xz} = \gamma_{yz} = 0$; $y = 0, b:\ w = \frac{\partial w}{\partial y} = \gamma_{xz} = \gamma_{yz} = 0$

Case 3. 2C2S edge condition: $x = 0, a:\ w = M_x = \gamma_{yz} = 0$; $y = 0, b:\ w = \frac{\partial w}{\partial y} = \gamma_{xz} = \gamma_{yz} = 0$

Case 4. 2S2C edge condition: $x = 0, a:\ w = \frac{\partial w}{\partial x} = \gamma_{xz} = \gamma_{yz} = 0;\quad y = 0, b:\ w = M_y = \gamma_{xz} = 0$

For thermal buckling:

In addition to the above boundary conditions, the following edge condition is to be imposed:

$$x = 0, a:\ u = v = 0\,;\ y = 0, b:\ u = v = 0$$

BUCKLING ANALYSIS

The conventional Raleigh-Ritz method of minimization of total potential energy V will be used in the buckling analysis.

Panel Deformation Functions

For an eigenvalue solution via the Rayleigh-Ritz method, the trial functions for the sandwich panel deformation $\{w, \gamma_{xz}, \gamma_{yz}\}$, satisfying the boundary conditions, may be expressed in the following double Fourier series:

Case 1. 4S edge condition (ref. 9)

$$w(x,y) = \sum_{m=1}^{\infty}\sum_{n=1}^{\infty} A_{mn} \sin\frac{m\pi x}{a} \sin\frac{n\pi y}{b} \tag{9}$$

$$\gamma_{xz}(x,y) = \sum_{m=1}^{\infty}\sum_{n=1}^{\infty} B_{mn} \cos\frac{m\pi x}{a} \sin\frac{n\pi y}{b} \tag{10}$$

$$\gamma_{yz}(x,y) = \sum_{m=1}^{\infty}\sum_{n=1}^{\infty} C_{mn} \sin\frac{m\pi x}{a} \cos\frac{n\pi y}{b} \tag{11}$$

Case 2. 4C edge condition (ref. 15)

$$w(x,y) = \sin\frac{\pi x}{a} \sin\frac{\pi y}{b} \sum_{m=1}^{\infty}\sum_{n=1}^{\infty} A_{mn} \sin\frac{m\pi x}{a} \sin\frac{n\pi y}{b} \tag{12}$$

$$\gamma_{xz}(x,y) = \cos\frac{\pi x}{a} \sin\frac{\pi y}{b} \sum_{m=1}^{\infty}\sum_{n=1}^{\infty} B_{mn} \sin\frac{m\pi x}{a} \sin\frac{n\pi y}{b} + \sin\frac{\pi x}{a} \sin\frac{\pi y}{b} \sum_{m=1}^{\infty}\sum_{n=1}^{\infty} mB_{mn} \cos\frac{m\pi x}{a} \sin\frac{n\pi y}{b} \tag{13}$$

$$\gamma_{yz}(x,y) = \sin\frac{\pi x}{a} \cos\frac{\pi y}{b} \sum_{m=1}^{\infty}\sum_{n=1}^{\infty} C_{mn} \sin\frac{m\pi x}{a} \sin\frac{n\pi y}{b} + \sin\frac{\pi x}{a} \sin\frac{\pi y}{b} \sum_{m=1}^{\infty}\sum_{n=1}^{\infty} nC_{mn} \sin\frac{m\pi x}{a} \cos\frac{n\pi y}{b} \tag{14}$$

Case 3. 2C2S edge condition (ref. 15)

$$w(x,y) = \sin\frac{\pi y}{b} \sum_{m=1}^{\infty}\sum_{n=1}^{\infty} A_{mn} \sin\frac{m\pi x}{a} \sin\frac{n\pi y}{b} \tag{15}$$

$$\gamma_{xz}(x,y) = \sin\frac{\pi y}{b} \sum_{m=1}^{\infty}\sum_{n=1}^{\infty} B_{mn} \cos\frac{m\pi x}{a} \sin\frac{n\pi y}{b} \tag{16}$$

$$\gamma_{yz}(x,y) = \cos\frac{\pi y}{b} \sum_{m=1}^{\infty}\sum_{n=1}^{\infty} C_{mn} \sin\frac{m\pi x}{a} \sin\frac{n\pi y}{b} + \sin\frac{\pi y}{b} \sum_{m=1}^{\infty}\sum_{n=1}^{\infty} nC_{mn} \sin\frac{m\pi x}{a} \cos\frac{n\pi y}{b} \tag{17}$$

Case 4. 2S2C edge condition (ref. 15)

$$w(x,y) = \sin\frac{\pi x}{a} \sum_{m=1}^{\infty}\sum_{n=1}^{\infty} A_{mn} \sin\frac{m\pi x}{a} \sin\frac{n\pi y}{b} \tag{18}$$

$$\gamma_{xz}(x,y) = \cos\frac{\pi x}{a} \sum_{m=1}^{\infty}\sum_{n=1}^{\infty} B_{mn} \sin\frac{m\pi x}{a} \sin\frac{n\pi y}{b} + \sin\frac{\pi x}{a} \sum_{m=1}^{\infty}\sum_{n=1}^{\infty} mB_{mn} \cos\frac{m\pi x}{a} \sin\frac{n\pi y}{b} \tag{19}$$

$$\gamma_{yz}(x,y) = \sin\frac{\pi x}{a} \sum_{m=1}^{\infty}\sum_{n=1}^{\infty} C_{mn} \sin\frac{m\pi x}{a} \cos\frac{n\pi y}{b} \tag{20}$$

Uniform Temperature (Zero Thermal Moments)

It is well known that thermal stresses are not caused by external loads but are the consequences of restrained thermal distortion. The intensities of thermal stresses will change when a structure is deformed; therefore, the thermal stress levels are the functions of strains. In classical thermal buckling of a structural panel (under uniform temperature rise with constrained edges), the first-order lateral deflections of the panel will cause only second-order small changes in the in-plane strains (thus, thermal stresses) at the onset of thermal buckling (ref. 28). In mechanical buckling, however, the external loads are held constant during buckling. If the second-order effect is neglected, then the in-plane thermal loads may be considered constant during thermal buckling. Thus thermal buckling problems would be equivalent to mechanical buckling problems; therefore, the conventional methods of structural stability analysis may be applied to the thermal buckling analysis.

The buckling equations will be developed first for the mechanical buckling under the combined loading condition $\{N_x \to -N_x,\ N_y \to -N_y,\ N_{xy} \to -N_{xy}\}$. The resulting mechanical buckling equation could then be applied directly to the thermal buckling of the sandwich panels with constraint edges under uniform panel temperature (i.e., $\{N_x = -N_x^T,\ N_y = -N_y^T,\ N_{xy} = -N_{xy}^T\}$, $\{M_x^T,\ M_y^T,\ M_{xy}^T\} = 0$, $u = v = w = 0$).

Characteristic Equations in Terms of Load Factors

After substituting the trial deformation functions (eqs. (9) through (20)) into the energy equations for V_1 (eq. (7)) and V_2 (eq. (8)) (signs of forcing functions reversed), and after performing the double integrations, the components of V_1 and V_2 may be calculated for different indicial conditions under different panel edge conditions (ref. 29).

Substituting V_1 and V_2 expressed in terms of Fourier coefficients A_{mn}, B_{mn} and C_{mn} (ref. 29) into V, and then minimizing V with respect to each of $\{A_{mn},\ B_{mn},\ \text{and}\ C_{mn}\}$ according to the Rayleigh-Ritz principle,

$$\frac{\partial V}{\partial A_{mn}} = \frac{\partial V}{\partial B_{mn}} = \frac{\partial V}{\partial C_{mn}} = 0 \tag{21}$$

one obtains three homogeneous simultaneous equations (i.e., characteristic equations) for each indicial set of $\{m, n\}$. Those three equations may be combined into one characteristic equation containing only the panel deflection coefficient $A_{k\ell}$. Namely,

$$\sum_{k=1}^{\infty}\sum_{\ell=1}^{\infty}\left[\frac{M_{mnk\ell}}{k_{xy}}+\delta_{mnk\ell}\right]A_{k\ell}=0 \tag{22}$$

where the stiffness/geometry parameter $M_{mnk\ell}$ appearing in equation (22) is defined as

$$M_{mnk\ell}\equiv\frac{1}{\eta}\frac{ab}{D^*}\left(\frac{a}{\pi}\right)^2\left[\underbrace{a^{11}_{mnk\ell}}_{\substack{\text{classical}\\ \text{thin plate}\\ \text{theory term}}}+\underbrace{\frac{a^{12}_{mnk\ell}\left(a^{23}_{mnk\ell}a^{31}_{mnk\ell}-a^{21}_{mnk\ell}a^{33}_{mnk\ell}\right)}{a^{22}_{mnk\ell}a^{33}_{mnk\ell}-a^{23}_{mnk\ell}a^{32}_{mnk\ell}}}_{\text{transverse shear effect terms}}+\underbrace{\frac{a^{13}_{mnk\ell}\left(a^{21}_{mnk\ell}a^{32}_{mnk\ell}-a^{22}_{mnk\ell}a^{31}_{mnk\ell}\right)}{a^{22}_{mnk\ell}a^{33}_{mnk\ell}-a^{23}_{mnk\ell}a^{32}_{mnk\ell}}}_{\text{transverse shear effect terms}}\right] \tag{23}$$

where the coefficients $a^{ij}_{mnk\ell}$ $(i, j = 1, 2, 3)$ are the partial functions of $\{D_{ij}, D_{Qx}, D_{Qy}, m, n, a, b, k_x, k_y\}$ and their functional forms vary with indicial and edge conditions. For the 4S, 4C, 2C2S, and 2S2C edge conditions there are 1, 9, 3, and 3 different sets of $a^{ij}_{mnk\ell}$, respectively, and these are defined in reference 29.

In equation (23) η is a numerical parameter, and in equation (22) $\delta_{mnk\ell}$ is a special delta function which is nonzero only when $m \pm k =$ odd, and $n \pm \ell =$ odd.

Case 1. 4S edge condition

$$\begin{cases}\eta = 32\\ \delta_{mnk\ell}=\dfrac{mnk\ell}{(m^2-k^2)(n^2-\ell^2)}\ ;\ m\pm k=\text{odd}, n\pm\ell=\text{odd}\end{cases} \tag{24}$$

Case 2. 4C edge condition

$$\begin{cases}\eta=\frac{(16)^3}{2}\ ;\ \delta_{mnk\ell}=\\ \dfrac{mnk\ell[m^2+k^2-2][n^2+\ell^2-2]}{(m^2-k^2)(n^2-\ell^2)[(m+k)^2-4][(m-k)^2-4][(n+\ell)^2-4][(n-\ell)^2-4]}\ ;\\ m\pm k=\text{odd}, n\pm\ell=\text{odd}\end{cases} \tag{25}$$

Case 3. 2C2S edge condition

$$\begin{cases}\eta = 8^3\\ \delta_{mnk\ell}=\dfrac{mnk\ell[2-(n^2+\ell^2)]}{(m^2-k^2)(n^2-\ell^2)[(n+\ell)^2-4][(n-\ell)^2-4]}\ ;\\ m\pm k=\text{odd}, n\pm\ell=\text{odd}\end{cases} \tag{26}$$

Case 4. 2S2C edge condition

$$\begin{cases}\eta = 8^3\\ \delta_{mnk\ell}=\dfrac{mnk\ell[2-(m^2+k^2)]}{(m^2-k^2)(n^2-\ell^2)[(m+k)^2-4][(m-k)^2-4]}\ ;\\ m\pm k=\text{odd}, n\pm\ell=\text{odd}\end{cases} \tag{27}$$

The characteristic equation (22) forms a system of infinite number of simultaneous homogeneous equations (i.e., one infinite series equation for each set of $\{m, n\}$ values). Because there is no coupling between the even case (symmetric buckling) and the odd case (antisymmetric buckling) (ref. 9), those simultaneous homogeneous equations may be divided into two groups that are independent of each other: one group in which $m \pm n$ is even, and the other group in which $m \pm n$ is odd (refs. 9, 13, 14).

For the deflection coefficients $A_{k\ell}$ to have nontrivial solutions under the assigned values of $\{k_x, k_y, \frac{b}{a}\}$, the determinant of coefficients of unknown $A_{k\ell}$ of the simultaneous homogeneous equations generated from equation (22) must vanish. The largest eigenvalue $1/k_{xy}$ thus obtained will give the lowest shear buckling load factor k_{xy} for given values $\{k_x, k_y, \frac{b}{a}\}$. When the transverse shear effect is neglected (eqs. (22), (23)), $\{k_x, k_y, k_{xy}\}$ are a function only of $\frac{b}{a}$, and independent of panel size. However, they will become panel-size dependent if the transverse shear effect is considered.

In the actual eigenvalue computations, the determinants of order 12 were found to give sufficiently accurate eigenvalue solutions (ref. 9). These determinants are given in reference 29 for the cases $m \pm n =$ even (symmetric buckling) and $m \pm n =$ odd (antisymmetric buckling) for different edge conditions.

Characteristic Equations in Terms of Temperature

For thermal buckling, the main objective is to find the buckling temperature, T_{cr}, rather than thermal buckling loads. Therefore, equation (22) needs to be rewritten in terms of temperature rather than load factors. For the uniform temperature case, the thermal forces have the following forms:

$$\begin{aligned}N_x^T &= \left(\bar{A}_{11}\alpha_x+\bar{A}_{12}\alpha_y\right)T\\ N_y^T &= \left(\bar{A}_{21}\alpha_x+\bar{A}_{22}\alpha_y\right)T\\ N_{xy}^T &= \bar{A}_{66}\alpha_{xy}T\end{aligned} \tag{28}$$

which were obtained from equations (4) and (6) setting $T_1 = T_2 = T$.

The coefficient $a^{11}_{mnk\ell}$ appearing in equation (23) contains thermal forcing terms (ref. 29). Thus, $a^{11}_{mnk\ell}$ may be written in two parts as

$$a^{11}_{mnk\ell}=\bar{a}^{11}_{mnk\ell}+\left[\xi(m,k)N_x^T+\zeta(n,\ell)N_y^T\right] \tag{29}$$

where $\bar{a}^{11}_{mnk\ell}$ is the first part of $a^{11}_{mnk\ell}$ without the thermal forcing terms, $\xi(m, k)$ and $\zeta(n, \ell)$ are, respectively, the numerical coefficients of N_x^T and N_y^T, whose values change with the indicial and the edge conditions.

In light of equation (29), equation (22) could be rewritten as

$$\sum_{k=1}^{\infty}\sum_{\ell=1}^{\infty}\left[\frac{\overline{M}_{mnk\ell}}{T}+P_{mnk\ell}+\delta_{mnk\ell}\right]A_{k\ell}=0 \tag{30}$$

where $\overline{M}_{mnk\ell}$ is the modified $M_{mnk\ell}$ in which $a^{11}_{mnk\ell}$ is replaced with $\overline{a}_{mnk\ell}$, and

$$P_{mnk\ell} \equiv \frac{ab}{\eta A_{66}\alpha_{xy}}\Big[\xi(m,k)(\bar{A}_{11}\alpha_x + \bar{A}_{12}\alpha_y) + \zeta(n,\ell)(\bar{A}_{21}\alpha_x + \bar{A}_{22}\alpha_y)\Big] \quad (31)$$

In equation (30), both $\overline{M}_{mnk\ell}$ and $P_{mnk\ell}$ terms contain material properties that are temperature dependent. Thus, in the eigenvalue solution process using equation (30), one has to assume a temperature T_a and use the corrresponding material properties as inputs to calculate the eigenvalue $1/T_{cr}$ where T_{cr} is the buckling temperature. This iteration process must be continued until the assumed temperature T_a approaches the buckling temperature T_{cr}.

Thus, in thermal buckling, the eigenvalue solution process requires a temperature iteration process and, therefore, is slightly different from that in mechanical buckling for which only a one-step eigenvalue solution process is needed.

Different Face-Sheet Temperatures (Nonzero Thermal Moments)

When face-sheet temperatures are different (i.e., $T_1 \neq T_2$), the sandwich panel will be subjected not only to thermal forces $\{N^T_x, N^T_y, N^T_{xy}\}$ but also to thermal moments $\{M^T_x, M^T_y, M^T_{xy}\}$. The problem then becomes a bending one and no longer an eigenvalue problem. The panel deflection w can then be calculated in terms of Fourier coefficient A_{mn}. The buckling condition will correspond to that when the term in series representation of w (associated with a particular buckling mode shape) becomes unbounded (i.e., $A_{mn} \to \infty$ for a given $\{m,n\}$). For this case the 4S edge condition will be analyzed as an example.

Thermal Moments

Let the thermal moments $\{M^T_x, M^T_y, M^T_{xy}\}$ be expressed in double Fourier series in accordance with the deformation functions given in equations (9) to (11) as

$$M^T_x = \sum_{m=1}^{\infty}\sum_{n=1}^{\infty} F_{mn}\sin\frac{m\pi x}{a}\sin\frac{n\pi y}{b} \quad (32)$$

$$M^T_y = \sum_{m=1}^{\infty}\sum_{n=1}^{\infty} H_{mn}\sin\frac{m\pi x}{a}\sin\frac{n\pi y}{b} \quad (33)$$

$$M^T_{xy} = \sum_{m=1}^{\infty}\sum_{n=1}^{\infty} S_{mn}\cos\frac{m\pi x}{a}\cos\frac{n\pi y}{b} \quad (34)$$

where the Fourier coefficients F_{mn}, H_{mn}, S_{mn} are given by

$$F_{mn} = \frac{4}{ab}\int_o^a\int_o^b M^T_x \sin\frac{m\pi x}{a}\sin\frac{m\pi y}{b}dxdy \quad (35)$$

$$H_{mn} = \frac{4}{ab}\int_o^a\int_o^b M^T_y \sin\frac{m\pi x}{a}\sin\frac{m\pi y}{b}dxdy \quad (36)$$

$$S_{mn} = \frac{4}{ab}\int_o^a\int_o^b M^T_{xy} \cos\frac{m\pi x}{a}\cos\frac{n\pi y}{b}dxdy \quad (37)$$

In light of the deformation functions (eqs. (9) to (11)) and the thermal moment expressions (eqs. (32) to (34)), the energy equations (7) (setting $u = v = 0$) and (8) may be integrated to yield the forms given in reference 29. The thermal moment terms turned out to be linear functions of A_{mn}, B_{mn}, or C_{mn}, and not quadratic functions of $\{A_{mn}, B_{mn}, C_{mn}\}$ in the energy expressions (ref. 29).

Nonhomogeneous Equations

After the application of the Rayleigh-Ritz method according to equation (21), one obtains three nonhomogeneous simultaneous equations for each indicial set of $\{m,n\}$, which may be combined to yield one equation in terms of $A_{k\ell}$ (ref. 29):

$$\frac{M_{mnmn}}{k_{xy}}A_{mn} + \sum_{k=1}^{\infty}\sum_{p=1}^{\infty}\delta_{mnk\ell}A_{k\ell} = R_{mnmn} \quad (38)$$

where M_{mnmn} is defined in equation (23) under the conditions m=k, n=ℓ, η=32, and the nonhomogeneous term R_{mnmn} is defined by

$$R_{mnmn} = \frac{1}{32k_{xy}}\frac{ab}{D^*}\left(\frac{a}{\pi}\right)^2 \left[J_{mn} - \frac{a^{12}_{mnmn}(K_{mn}a^{33}_{mnmn} - L_{mn}a^{23}_{mnmn})}{a^{22}_{mnmn}a^{33}_{mnmn} - a^{23}_{mnmn}a^{32}_{mnmn}} + \frac{a^{13}_{mnmn}(K_{mn}a^{32}_{mnmn} - L_{mn}a^{22}_{mnmn})}{a^{22}_{mnmn}a^{33}_{mnmn} - a^{23}_{mnmn}a^{32}_{mnmn}}\right] \quad (39)$$

where J_{mn}, K_{mn}, and L_{mn} are defined as

$$J_{mn} \equiv F_{mn}\left(\frac{m\pi}{a}\right)^2 + H_{mn}\left(\frac{n\pi}{b}\right)^2 - 2S_{mn}\left(\frac{m\pi}{a}\right)\left(\frac{n\pi}{b}\right) \quad (40)$$

$$K_{mn} \equiv -F_{mn}\left(\frac{m\pi}{a}\right) + S_{mn}\left(\frac{n\pi}{b}\right) \quad (41)$$

$$L_{mn} \equiv -H_{mn}\left(\frac{m\pi}{a}\right) + S_{mn}\left(\frac{n\pi}{b}\right) \quad (42)$$

Equation (38) forms an infinite number of nonhomogeneous simultaneous equations, each of which is associated with a set of $\{m,n\}$ values (or mode shape) for the calculation of an infinite number of Fourier (or Ritz) coefficients A_{mn} in the series representation of panel deflection $w(x,y)$ (eq. (9)).

Buckling Condition

The calculated Ritz coefficients A_{mn} have the following functional form:

$$A_{mn} = \frac{[\ ]_{mn}}{\Delta} \quad (43)$$

where the numerator $[\quad]_{mn}$ contains $\{M_{mnmn}, R_{mnmn}, \delta_{mnkl}\}$, and the denominator Δ is the determinant of the coefficients of A_{kl} of the nonhomogeneous simultaneous equations written out from equation (38). The detailed expressions of Δ of order 12 is shown in references 9 through 11 and 29 for either symmetrical or antisymmetrical buckling.

The mathematical meaning of the buckling state in light of equation (43) is that the Ritz coefficient A_{mn} becomes unbounded (i.e., infinite panel deflection, or $\Delta \to 0$). That is, when the buckling state is reached, the term in the series (eq. (9)) that corresponds to the particular deformation mode shape becomes the most important term.

From the above analysis, one sees that the buckling conditions for the cases with and without the thermal moments are identical (i.e., $\Delta = 0$) under the classical small deformation theory. Because of this finding, similar bending analyses for nonzero thermal moments for other edge conditions were not carried out.

NUMERICAL EXAMPLES

Physical Properties of Sandwich Panels

The sandwich panel is assumed to be fabricated with titanium face sheets and titanium honeycomb core, having the following geometrical and material properties:

Geometry: $h = 1.2$ in.; $t_s = 0.032$ in.; $a = a_o = 24$ in. (for varying b), or $ab = a_o^2$ (for constant panel area)

Material properties:

Face sheets

	70 °F	1000 °F
$E_x = E_y$, lb/in^2	16×10^6	10.5×10^6
G_{xy}, lb/in^2	6.2×10^6	4.7×10^6
$\nu_{xy} = \nu_{yx}$	0.31	0.31
$\alpha_x = \alpha_y$, in/in-°F	4.85×10^{-6}	5.6×10^{-6}
α_{xy}, in/in-°F	0	0

Honeycomb core (properties at 600 °F)

$$G_{Cyz} = 0.81967 \times 10^5 \text{ lb/in}^2$$
$$G_{Czx} = 1.81 \times 10^5 \text{ lb/in}^2$$

Buckling Interaction Curves

In generating the data for plotting the buckling interaction curves, k_y was set to zero. For a given $\frac{b}{a}$, different values of k_x were assigned; then the corresponding eigenvalues $1/k_{xy}$ were calculated from equation (22). Typical buckling interaction curves plotted in k_x-k_{xy} space for square panel ($\frac{b}{a} = 1$) are shown in figure 4. The additional set of buckling interaction curves shown in broken curves is for the case when the effect of transverse shear is neglected. For the square panels, the buckling interaction curves for 4S, 2S2C, and 4C cases are continuous curves of symmetric buckling. However, for the 2C2S case, the buckling interaction curves are composite curves, partly for symmetric buckling and partly for antisymmetric buckling. Notice that the effect of the transverse shear is quite large for the sandwich panel. Without a consideration of the transverse shear effect, the sandwich panel buckling strength could be overpredicted considerably. The 4S case has the lowest buckling strength. Through clamping two opposite edges (i.e., from 4S case to 2C2S and 2S2C cases), the buckling strength could be enhanced considerably. By additional clamping of the other two opposite edges (i.e., from 2C2S and 2S2C cases to 4C case), further improvement of the buckling strength could be achieved. However, the improvement is not as large as that for the previous case (i.e., from 4S case to 2C2S and 2S2C cases). With or without a consideration of the transverse shear effect, the improvement of buckling strength through edge clampings is larger in pure compression than in pure shear.

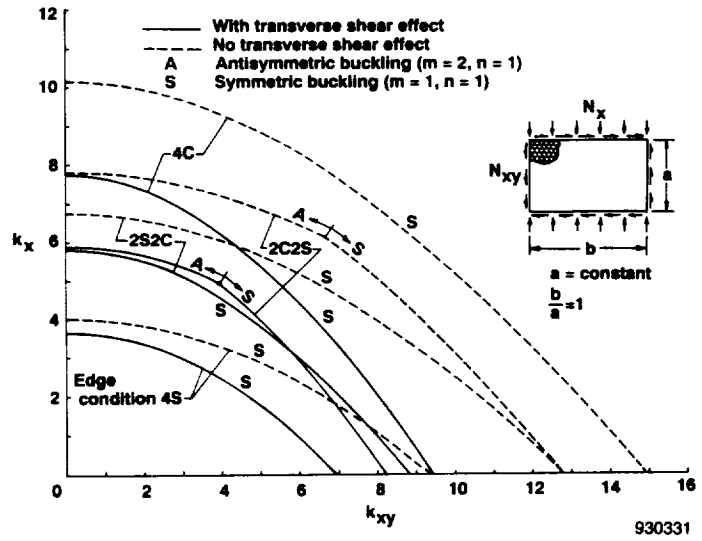

Fig. 4. Combined load buckling interaction plots for a honeycomb-core sandwich panel under different edge conditions.

Buckling Interaction Surfaces

By using families of buckling interaction curves generated for different values of $\frac{b}{a}$ (a = constant) and for different edge conditions, three-dimensional buckling surfaces were constructed in $[k_x, k_{xy}, \frac{b}{a}]$ space as shown in figure 5. In the figure, the domains of symmetric and antisymmetric buckling (lowest buckling modes) are also shown. Figure 5 shows better visualization of the buckling behavior of the sandwich panel than the traditional buckling plots of k_x as a function of $\frac{b}{a}$, and k_{xy} as a function of $\frac{b}{a}$. For slender rectangular panels (i.e., $\frac{b}{a} < 1$), antisymmetric bucklings occur mostly in the compression-dominated regions. For wider panels (i.e., $\frac{b}{a} > 1$), the antisymmetric bucklings take place in the shear-dominated regions. In the neighborhood of $\frac{b}{a} = 1$, the lowest buckling modes are all symmetric (i.e., $m = 1$, $n = 1$) for the 4S, 4C and 2S2C cases, and only for the 2C2S case, the

lowest buckling mode in the compression-dominated region is antisymmetric (i.e., $m = 2$, $n = 1$). Such buckling behavior also occurs in the flat rectangular plates of $\frac{b}{a} \approx 1$.

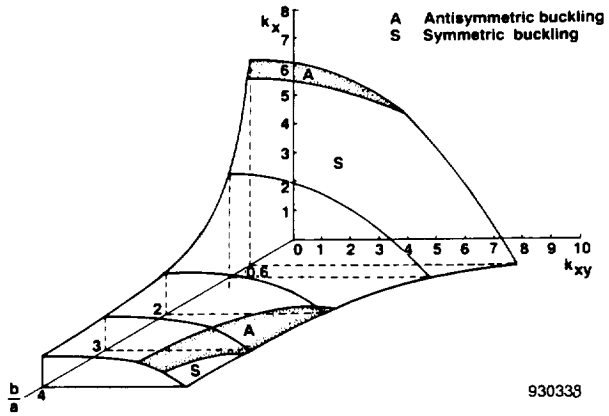

(a) Four edges simply supported (4S).

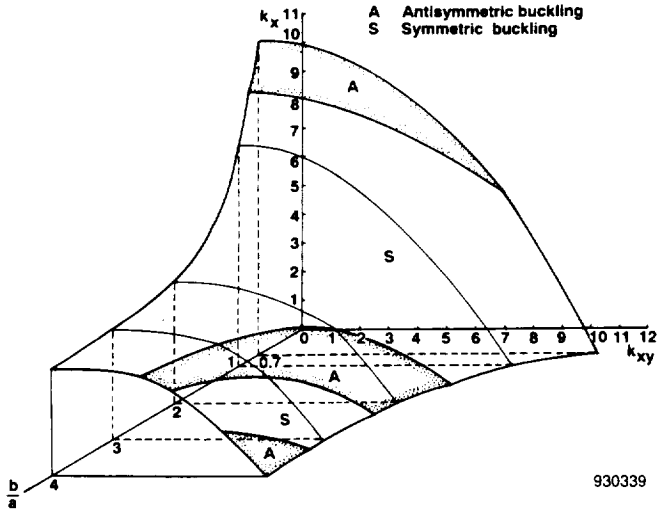

(b) Four edges clamped (4C).

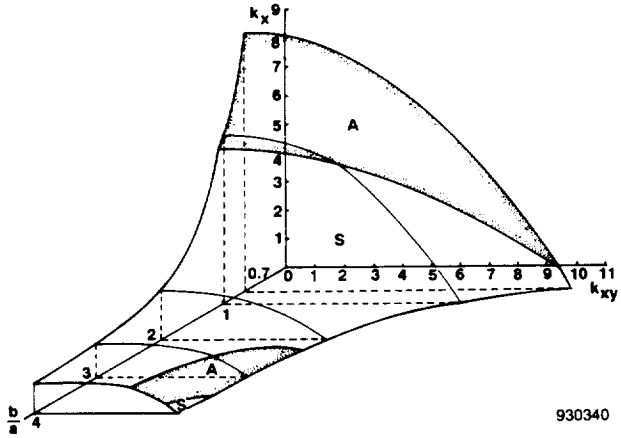

(c) Two sides clamped, two ends simply supported (2C2S).

Fig. 5. Buckling interaction surfaces for honeycomb-core sandwich panels under different edge conditions (a = constant).

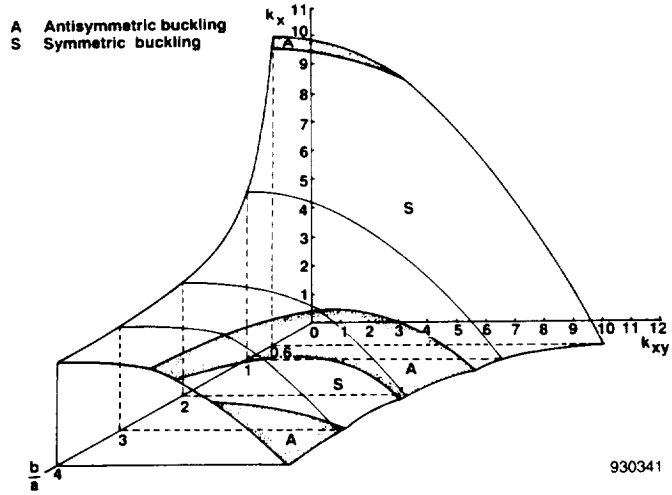

(d) Two sides simply supported, two ends clamped (2S2C).

Fig. 5. Concluded.

Buckling Curves for Pure Compression and Pure Shear

The buckling surfaces shown in figure 5 were constructed under the condition a = constant, and may not serve as ideal design plots for aerospace structural panels, because, when $\frac{b}{a}$ is changed (under a = constant), the panel weight (i.e., panel area ab) also is changed accordingly. In the aerospace structural designs, the main objective is the structural optimization. That is, for a given panel weight, the objective is to search for a panel with optimum buckling strengths (or stiffnesses). For this reason, modified buckling load factors $\bar{k}_x$ and $\bar{k}_{xy}$ ($\bar{k}_y = 0$) were recalculated as functions of $\frac{b}{a}$ under the condition $ab = a_o^2$ = constant (instead of a = constant). Figures 6 and 7, respectively, show the alternative plots of $\bar{k}_x$ as a function of $\frac{b}{a}$ for pure compression and $\bar{k}_{xy}$ as a function of $\frac{b}{a}$ for pure shear when the panel area ab was kept unchanged. In practical applications, the panel has to be supported by an edge frame (cross section assumed constant); therefore, the edge frame weight (or edge frame length, $(a + b)/2a_o$) was also plotted in figures 6 and 7 as a function of $\frac{b}{a}$. The square panel ($\frac{b}{a} = 1$) has the minimum edge frame weight; however, it does not have the optimum buckling strengths both in compression and shear. The compressive buckling strengths (fig. 6) reached minimum at $\frac{b}{a} = 1.6$, 1.4, 2.2, and 1.0, respectively, for the 4S, 4C, 2C2S, and 2S2C cases. The lowest shear buckling strengths (fig. 7) occur at $\frac{b}{a} = 0.9$, 0.9, 1.2, and 0.7, respectively, for the 4S, 4C, 2C2S, and 2S2C cases. Figures 6 and 7 serve as design curves for selecting the desired sandwich panel geometry (i.e., $\frac{b}{a}$ value). To boost the panel buckling strengths both in compression and shear, some weight penalty resulting from

the edge frame is inevitable. The desirable high stiffness-to-weight-ratio panel shapes will be slightly slender ($\frac{b}{a} < 1$), especially in light of the compressive buckling strength.

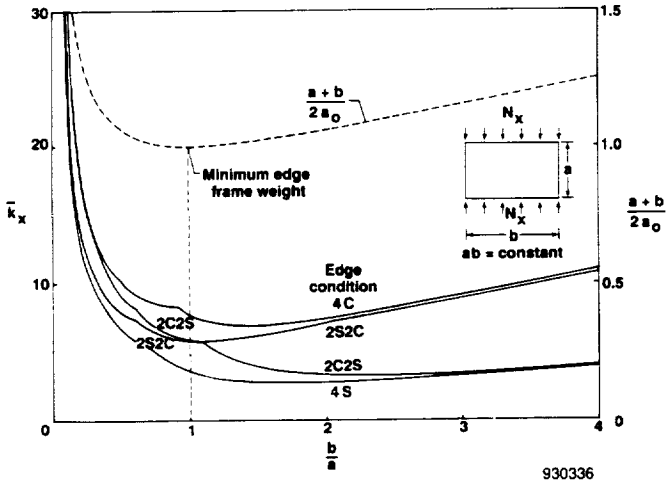

Fig. 6. Comparison of compressive buckling strengths of honeycomb-core sandwich panels under different edge conditions (constant panel areas).

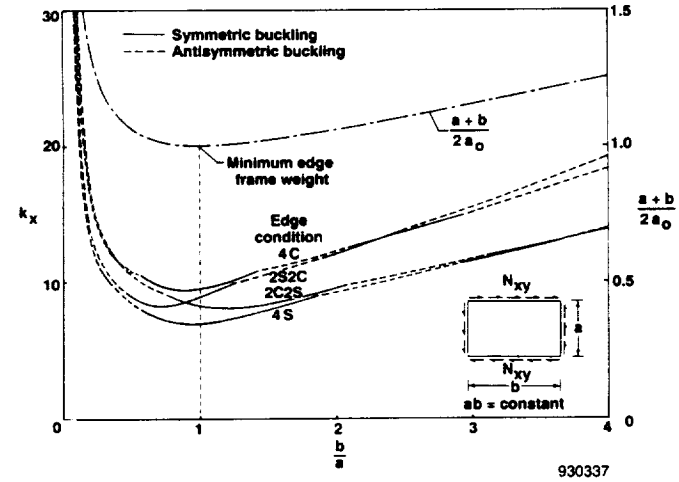

Fig. 7. Comparison of shear buckling strengths of honeycomb-core sandwich panels under different edge conditions (constant panel areas).

Thermal Buckling Curves

For most of the practical materials, the coupling coefficient of thermal expansion α_{xy} is zero. Therefore, in generating the data for thermal buckling curves, the following conditions were imposed: $\alpha_x = \alpha_y$, $\alpha_{xy} = 0$ (i.e., $N_{xy}^T = M_{xy}^T = 0$), $M_x^T = M_y^T = 0$.

These conditions will induce in-plane biaxial thermal compression without shear and bending. Figure 8 shows the buckling temperature, T_{cr}, plotted as a function of $\frac{b}{a}$, with the panel length a kept constant. Those thermal (biaxial compression) buckling curves somewhat resemble the uniaxial compressive buckling (mechanical buckling) curves k_x as a function of $\frac{b}{a}$ shown in figure 5. For buckling temperatures higher than 1000 °F, the face sheet material property data at 1000 °F were used as inputs to equation (30) for T_{cr} calculations because of the lack of material property data at high temperatures. For the honeycomb core, the only available material property data at 600 °F had to be used as inputs for T_{cr} calculations. The buckling temperature T_{cr} was found to be relatively insensitive to the material property change with temperature.

For the present particular panel (i.e., dimensions chosen), the thermal buckling temperatures T_{cr} exceed the titanium melting point (3074 °F) at the low $\frac{b}{a}$ and gradually decrease with the increase of $\frac{b}{a}$. At high aspect ratios, T_{cr} for 4S and 2C2S cases level off at about 1000 °F (below superplastic temperature, 1650 °F), and for 4C and 2S2C cases, at temperatures slightly below the melting point.

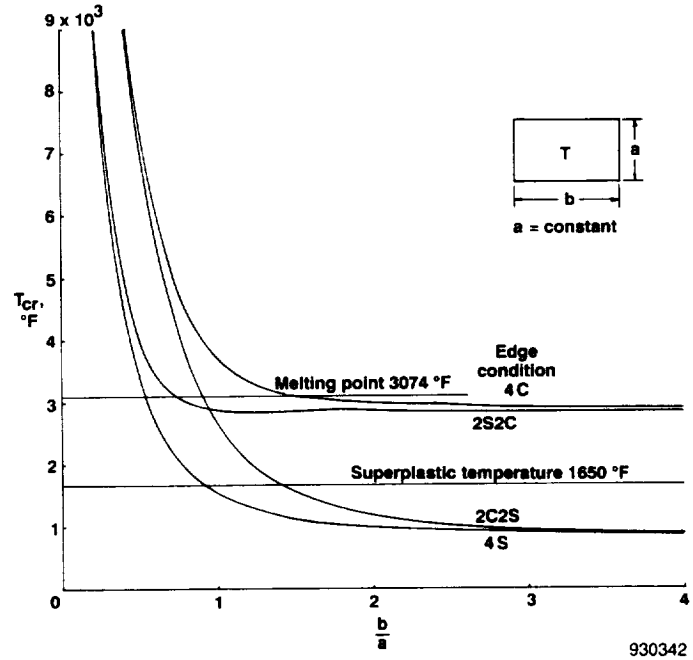

Fig. 8. Thermal buckling temperatures for honeycomb-core sandwich panels under different edge conditions (a = constant).

Figure 9 shows the alternative plots of T_{cr} as a function of $\frac{b}{a}$ for constant-area panels (i.e., ab = constant). The lowest buckling temperatures for 4S, 4C, 2C2S, and 2S2C cases are, respectively, at 1297 °F, 3702 °F (above melting point), 2194 °F (above superplastic temperature), and 2205 °F (above superplastic temperature) and occur, respectively, at $\frac{b}{a} = 1.0$, 0.975, 1.8, and 0.5.

For the present sandwich panel, the actual thermal buckling will take place only for the 4S case in the region $1.5 < \frac{b}{a} < 1.8$. Outside this region for the 4S case and for all

the range of $\frac{b}{a}$ for the other three edge conditions, no actual thermal buckling could occur because the sandwich panel will first undergo superplastic creep or melting.

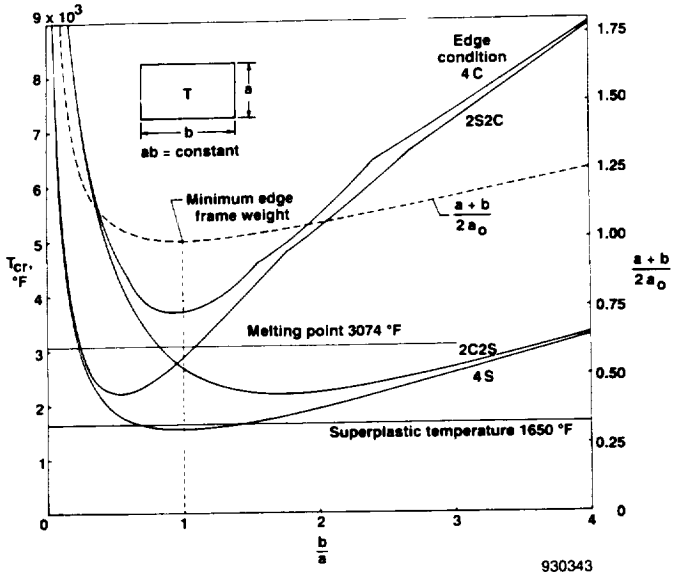

Fig. 9. Thermal buckling temperatures for honeycomb-core sandwich panels under different edge conditions (constant panel areas).

CONCLUDING REMARKS

By using the Rayleigh-Ritz method of minimizing the total potential energy of a structural system, the combined load (mechanical or thermal) buckling equations were established for orthotropic rectangular sandwich panels supported under four different edge conditions. Two-dimensional buckling interaction curves and three-dimensional buckling interaction surfaces were constructed for high-temperature honeycomb-core sandwich panels. The buckling interaction surfaces provide easy visualization of the variation of the panel buckling strengths and the domains of buckling modes (symmetric and antisymmetric) with the edge condition. Furthermore, the buckling temperature curves for the sandwich panels were presented.

The effect of transverse shear on the buckling strength is quite large for sandwich panels, and by neglecting the transverse shear effect, the buckling strengths could be overpredicted considerably. With the inclusion of the transverse shear effect, the buckling load factors became panel-size dependent in addition to panel-aspect-ratio dependent. Clamping the edges could enhance the buckling strength greatly more in compression than in shear. Thermal buckling conditions for the cases with and without thermal moments were found to be identical for the small deformation theory.*

*The author gratefully acknowledges the contributions by Barry Randall in setting up computer programs for the eigenvalue extractions.

REFERENCES

1. Tenney, D.R., W.B. Lisagor, and S.C. Dixon, "Materials and Structures for Hypersonic Vehicles," *J. Aircraft*, vol. 26, no. 11, Nov. 1989, pp. 953–970.

2. Jenkins, Jerald M., Leslie Gong, Robert D. Quinn, and Raymond L. Jackson, "Effect of Heat and Load on the Structure of a Mach 5-6 Class Inlet," NASP Technical Memorandum, NASP Joint Program Office, Wright-Patterson AFB, Ohio, 1991.

3. Venkateswaran, S., David W. Witte, and L. Roane Hunt, "Aerothermal Study in an Axial Compression Corner with Shock Impingement at Mach 6," AIAA 91-0527, Jan. 1991.

4. Ko, William L., John L. Shideler, and Roger A. Fields, *Buckling Characteristics of Hypersonic Aircraft Wing Tubular Panels*, NASA TM-87756, 1986.

5. Siegel, William H., *Experimental and Finite Element Investigation of the Buckling Characteristics of a Beaded Skin Panel for a Hypersonic Aircraft*, NASA CR-144863, 1978.

6. Ko, William L. and Raymond H. Jackson, *Compressive Buckling Analysis of Hat-Stiffened Panel*, NASA TM-4310, 1991.

7. Percy, W. and R. Fields, "Buckling Analysis and Test Correlation of Hat Stiffened Panels for Hypersonic Vehicles," AIAA 90-5219, Oct. 1990.

8. Ko, William L. and Raymond H. Jackson, *Thermal Behavior of a Titanium Honeycomb-Core Sandwich Panel*, NASA TM-101732, 1991.

9. Ko, William L. and Raymond H. Jackson, *Combined Compressive and Shear Buckling Analysis of Hypersonic Aircraft Structural Sandwich Panels*, NASA TM-4290, 1991. Also AIAA 92-2487-CP, Apr. 1992.

10. Ko, William L. and Raymond H. Jackson, *Combined-Load Buckling Behavior of Metal-Matrix Composite Sandwich Panels Under Different Thermal Environments*, NASA TM-4321, 1991.

11. Ko, William L. and Raymond H. Jackson, *Compressive and Shear Buckling Analysis of Metal Matrix Composite Sandwich Panels Under Different Thermal Environments*, NASA TM-4492, 1993.

12. Bert, Charles W. and K.N. Cho, "Uniaxial Compressive and Shear Buckling in Orthotropic Sandwich Plates by Improved Theory," AIAA 86-0977, May 1986.

13. Stein, Manuel and John Neff, *Buckling Stresses of Simply Supported Rectangular Flat Plates in Shear*, NACA TN-1222, 1947.

14. Batdorf, S.B. and Manuel Stein, *Critical Combinations of Shear and Direct Stress for Simply Supported Rectangular Flat Plates*, NACA TN-1223, 1947.

15. Green, A.E. and F.S. Hearmon, "The Buckling of Flat Rectangular Plywood Plates," Phil. Mag., ser. 7, vol. 36, no. 261, Oct. 1945, pp. 659–688.

16. Smith, R.C.T., "The Buckling of Plywood Plates in Shear," Australian Council for Aeronautics Report ACA-29, Oct. 1946.

17. Kuenzi, Edward W., W.S. Ericksen, and John J. Zahn, "Shear Stability of Flat Panels of Sandwich Construction," Forest Products Laboratory Report No. 1560, U.S. Forest Service, U.S. Department of Agriculture, 1962.

18. King, Carl S., "Stability of Flat, Clamped, Rectangular Sandwich Panels Subjected to Combined Inplane Loadings," University of Dayton Research Institute, Technical Report AF FDL-TR-76-137, Dec. 1976. Available from Air Force Wright Aeronautical Laboratories, Wright-Patterson AFB, Ohio 45433.

19. Hoff, N. J., "Buckling at High Temperature," *J. Roy. Aeronaut. Soc.*, vol. 61, Nov. 1957, pp. 756–774.

20. Klosner, J.M. and M.J. Forray, "Buckling of Simply Supported Plates Under Arbitrary Symmetrical Temperature Distributions," *J. Aeronaut. Sci.*, vol. 25, Mar. 1958, pp. 181–184.

21. Gossard, Myron L., Paul Seide, and William M. Roberts, *Thermal Buckling of Plates*, NACA TN-2771, 1952.

22. Siddaveere Gowda, R.M. and K.A.V. Pandalai, *Thermal Buckling of Orthotropic Plates*, Studies in Structural Mechanics, Hoff's 65th Anniversary Volume, Indian Institute of Technology, Madras-36, India, 1970, pp. 9–44.

23. Tauchert, T.R. and N.N. Huang, "Thermal Buckling and Postbuckling Behavior of Antisymmetric Angle-Ply Laminates," *Proc. Internat'l. Symp. Composite Materials and Structures*, Beijing, China, June 1986, pp. 357–362.

24. Tauchert, T.R. and N.N. Huang, "Thermal Buckling of Symmetric Angle-ply Laminated Plates," *Composite Structures*, I.H. Marshall (ed.), 1987, pp. 1424–1435.

25. Thangaratnam, Kari R., Palaninathan, and J. Ramachandran, "Thermal Buckling of Composite Laminated Plates," *Computers and Structures*, vol. 32, no. 5, 1989, pp. 1117–1124.

26. Huang, N.N. and T.R. Tauchert, "Postbuckling Response of Antisymmetric Angle-Ply Laminates to Uniform Temperature Loading," *Acta Mechanica*, vol. 72, 1988, pp. 173–183.

27. Tauchert, Theodore R., "Chapter 2, Thermal Stresses in Plates—Statical Problems," in *Thermal Stresses I*, Richard B. Hetnarski (ed.), Elsevier Sciences Publishing Co., New York, 1986, pp. 23–141.

28. Timoshenko, Stephen P. and James M. Gere, *Theory of Elastic Stability*, McGraw-Hill Book Co., New York, 1961, pp. 337–338, 344–346.

29. Ko, William L., *Mechanical and Thermal Buckling Analysis of Rectangular Sandwich Panels Under Different Edge Conditions*, NASA TM-4535 (in press).

REPORT DOCUMENTATION PAGE

Form Approved
OMB No. 0704-0188

1. AGENCY USE ONLY (Leave blank)	2. REPORT DATE	3. REPORT TYPE AND DATES COVERED
	October 1993	Technical Memorandum

4. TITLE AND SUBTITLE

Mechanical and Thermal Buckling Analysis of Sandwich Panels Under Different Edge Conditions

5. FUNDING NUMBERS

WU 505-63-40

6. AUTHOR(S)

William L. Ko

7. PERFORMING ORGANIZATION NAME(S) AND ADDRESS(ES)

NASA Dryden Flight Research Facility
P.O. Box 273
Edwards, California 93523-0273

8. PERFORMING ORGANIZATION REPORT NUMBER

H-1953

9. SPONSORING/MONOTORING AGENCY NAME(S) AND ADDRESS(ES)

National Aeronautics and Space Administration
Washington, DC 20546-0001

10. SPONSORING/MONITORING AGENCY REPORT NUMBER

NASA TM-4535

11. SUPPLEMENTARY NOTES

This paper was originally prepared for the Pacific International Conference on Aerospace Science and Technology (PICAST'1), Taiwan, Republic of China, Dec. 6–9, 1993.

12a. DISTRIBUTION/AVAILABILITY STATEMENT

Unclassified—Unlimited
Subject Category 24

12b. DISTRIBUTION CODE

13. ABSTRACT (Maximum 200 words)

By using the Rayleigh-Ritz method of minimizing the total potential energy of a structural system, combined load (mechanical or thermal load) buckling equations are established for orthotropic rectangular sandwich panels supported under four different edge conditions. Two-dimensional buckling interaction curves and three-dimensional buckling interaction surfaces are constructed for high-temperature honeycomb-core sandwich panels supported under four different edge conditions. The interaction surfaces provide easy comparison of the panel buckling strengths and the domains of symmetrical and antisymmetrical buckling associated with the different edge conditions. Thermal buckling curves of the sandwich panels also are presented. The thermal buckling conditions for the cases with and without thermal moments were found to be identical for the small deformation theory. In sandwich panels, the effect of transverse shear is quite large, and by neglecting the transverse shear effect, the buckling loads could be overpredicted considerably. Clamping of the edges could greatly increase buckling strength more in compression than in shear.

14. SUBJECT TERMS

Buckling interaction curves; Buckling interaction surfaces; Mechanical buckling; Sandwich panels; Thermal buckling

15. NUMBER OF PAGES

16

16. PRICE CODE

A03

17. SECURITY CLASSIFICATION OF REPORT	18. SECURITY CLASSIFICATION OF THIS PAGE	19. SECURITY CLASSIFICATION OF ABSTRACT	20. LIMITATION OF ABSTRACT
Unclassified	Unclassified	Unclassified	Unlimited